I&EC research
Industrial & Engineering Chemistry Research

Article

Cite This: Ind. Eng. Chem. Res. 2019, 58, 8681−8689

pubs.acs.org/IECR

Optimum Reaction Conditions for 1,4-Anhydroerythritol and Xylitol Hydrodeoxygenation over a ReO_x−Pd/CeO_2 Catalyst via Design of Experiments

Blake MacQueen,[†] Elizabeth Barrow,[†] Gerardo Rivera Castro,[‡] Yomaira Pagan-Torres,[‡] Andreas Heyden,[†] and Jochen Lauterbach*[,†]

[†]Department of Chemical Engineering, University of South Carolina, 541 Main Street, Columbia, South Carolina 29208, United States

[‡]Department of Chemical Engineering, University of Puerto Rico—Mayaguez Campus, Mayaguez, Puerto Rico 00681-9000, United States

Supporting Information

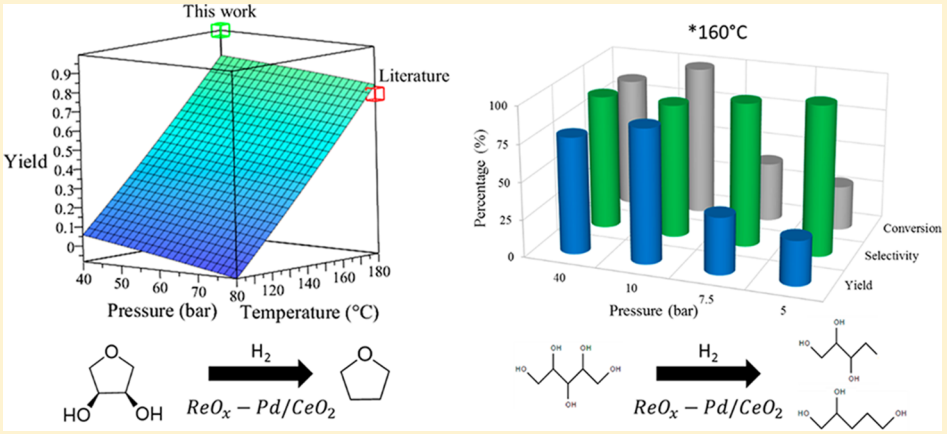

ABSTRACT: In this study, we demonstrate that for the simultaneous hydrodeoxygenation (HDO) of 1,4-anhydroerythritol a comparable yield of tetrahydrofuran is obtained at half the previously reported H_2 pressure. The simultaneous hydrodeoxygenation was conducted using a heterogeneous ReO_x−Pd/CeO_2 catalyst. An L9 Taguchi design of experiment was enacted to elucidate the temperature, pressure, and catalyst loading effects on the yield of the HDO reaction by testing pressures ranging from 40 to 80 bar H_2, temperatures of 100−180 °C, and Re loadings of 2−4 wt %. Our design showed that the yield of this reaction is significantly affected by the reaction temperature only. An L9 Taguchi design was conducted for xylitol simultaneous hydrodeoxygenation with pressures ranging from 5 to 10 bar H_2, temperatures of 140−180 °C, and Re loadings of 2−4 wt %. The xylitol design elucidated the direct relation of pressure, and the inverse relation of temperature and catalyst loading, to yield with the optimal reaction condition being 140 °C and 10 bar H_2.

INTRODUCTION

Lignocellulosic biomass is derived from cell walls and can be reformed into liquid phase and upgraded into sugars that contain hydroxyl groups, such as 1,4-anhydroerythritol (AHERY).[1−3] The liquid phase reforming produces glucose and can be fermented into erythritol. Erythritol can then go through an acid catalyzed dehydration to form AHERY.[4] These sugars can either undergo deoxydehydration to form double bonds or hydrodeoxygenation (HDO) to remove vicinal hydroxyl groups.[5] The removal of the hydroxyl groups allows for the biomass derived sugars to be utilized as an alternative feedstock for fuel and platform chemical production.[6] The deoxydehydration typically uses a ReO_x−Au/CeO_2 catalyst, and the HDO uses either a WO_x−Pd/ZrO_2 catalyst to remove a single hydroxyl group or a ReO_x−Pd/CeO_2 catalyst to simultaneously remove two vicinal hydroxyl groups.[4,5,7−10] The latter reaction is a simultaneous hydrodeoxygenation (S-HDO) and proceeds via deoxydehydration followed by a hydrogenation step that allows for the simultaneous removal of two vicinal hydroxyl groups. Re based catalysts have been utilized for deoxydehydration due to their high reaction rates and selectivity.[11] Deoxydehydration of methyl glycosides over these Re based catalysts has been achieved at low H_2 pressures with high yields.[10] Literature has shown that ReO_x−Pd/CeO_2 is a better catalyst for the S-HDO of AHERY as compared to

Received: March 15, 2019
Revised: May 2, 2019
Accepted: May 6, 2019
Published: May 6, 2019

DOI: 10.1021/acs.iecr.9b01463
Ind. Eng. Chem. Res. 2019, 58, 8681−8689

ReO_x−Pd on other oxide supports.[12] The S-HDO of AHERY, producing tetrahydrofuran (THF), was used as a model reaction for S-HDO since it has two vicinal *cis*-hydroxyl groups. AHERY is ideal to use for a model reaction for S-HDO since it can only occur once on this compound. For other compounds containing more than two vicinal *cis*-hydroxyl groups, the hydroxyl groups that the S-HDO selectively removes first dictate the possible products that can be formed. The AHERY S-HDO is shown in Scheme 1.

Scheme 1. Simultaneous Hydrodeoxygenation of 1,4-Anhydroerythritol to Tetrahydrofuran

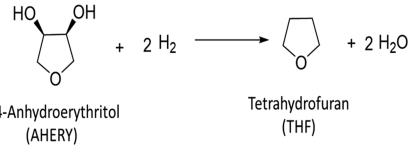

HDO reactions have been conducted over a wide range of conditions, including pressures that exceed 75 bar H_2 and temperatures over 350 °C.[13−26] One of the issues that arises with HDO reactions is that the conditions involve either high pressure, high temperature, or both high pressure and temperature. These harsh conditions challenge the scaling of aqueous-phase HDO reactions for commercial viability and have resulted in a bottleneck for further development of these processes.[27] Milder conditions for these HDO reactions would be more desirable and economically favorable for pilot scale and beyond. The AHERY S-HDO has been conducted in the literature at 80 bar and 180 °C.[12] For a batch process, these conditions would pose major problems at an industrial level regarding economic viability. A pressure of 80 bar H_2 greatly surpasses the safety rating for many commonly used industrial batch reactors. In this work, we investigated the feasibility of running this reaction at milder conditions that were optimized through a design of experiment. Our goal was to determine the main effects of pressure, temperature, and catalyst loading on the yield and to elucidate scalable operating conditions. These HDO reactions conducted at milder conditions could allow for scaling from the lab scale to the pilot scale and beyond to be easier and more economical. The ability to reduce heating and feedstock costs can directly improve the economic viability of these processes.

Xylitol is a common sugar substitute that is derived from lignocellulosic biomass and is already produced on a commercial scale. Lignocellulosic biomass can go through a hemicellulose extraction to obtain xylan which can then go through hydrolysis to form xylose.[28] The xylose can then be fermented into xylitol. Xylitol contains five vicinal hydroxyl groups which can undergo an HDO. The S-HDO of xylitol can produce 1,2-dideoxypentitol and 1,2,5-pentanetriol if one pair of vicinal hydroxyl groups is removed. Both 1,2-dideoxypentitol and 1,2,5-pentanetriol are considered value-added products and are used as chemical building blocks for various reactions. If another S-HDO occurs, the 1,2-dideoxypentitol and 1,2,5-pentanetriol are converted to either 1-pentanol or 3-pentanol. 1-Pentanol and 3-pentanol are widely used industrial chemicals; however, these are of low value when compared to the current production price of xylitol.

Xylitol S-HDO has been conducted in the literature at 160 °C and 80 bar H_2.[12] The reaction was conducted for 24 h and mainly produced 1-pentanol and 3-pentanol. In this work, we have determined mild and scalable reaction conditions for xylitol S-HDO to the value-added products 1,2-dideoxypentitol and 1,2,5-pentanetriol. The products initially formed in this reaction are between 300 and 5000 times more valuable than the initial xylitol. The pentanols are on the order of 1.2−3.3 times as valuable as the initial xylitol and require a longer reaction time to form. Thus, a shorter time scale will be used for evaluation and comparison between experimental runs to focus on the significant value-added products.

EXPERIMENTAL SECTION

Chemicals. The chemicals used in this work are listed in the Supporting Information in Table 1 Supplemental.

Catalyst Preparation. The various ReO_x−Pd/CeO_2 catalysts were prepared via wet impregnation using the procedure described by Ota et al.[5] The CeO_2 support was first calcined at 600 °C for 3 h. ReO_x was added to the support with an aqueous solution of ammonium perrhenate (NH_4ReO_4). Catalysts were prepared with 2, 3, and 4 wt % Re. The catalyst was then dried at 110 °C for 12 h. The Pd was then impregnated with an aqueous solution of palladium(II) nitrate ($Pd(NO_3)_2$) and dried in air at 110 °C for 12 h. Following the drying, the catalysts were calcined in air at 500 °C for 3 h. After calcination, the catalysts were ground into a powder. The molar ratio between Pd and Re was kept constant at Pd/Re = 0.25 (which corresponds to the weight percent ratio of Pd/Re = 0.15) for the various catalyst loadings.

Catalyst Characterization. The ReO_x−Pd/CeO_2 catalysts were characterized using X-ray diffraction (XRD), inductively coupled plasma optical emission spectroscopy (ICP-OES), and temperature-programmed reduction (TPR). The characterization results are shown in Figure 1 Supplemental. XRD was conducted with a Rigaku MiniFlex II with Cu Kα source radiation (α = 1.5406) scanning between 2θ of 10° and 2θ of 80° at a rate of 2 deg/min. The XRD spectra for the catalysts match the spectra for cerianite reported previously in the literature.[12] No solid Re peaks were observed in the XRD patterns, which implies that our Re particles are well-dispersed on our catalyst surface. To determine the actual weight loadings of our catalysts, ICP-OES was conducted on a PerkinElmer Optima 2000 DV optical emission spectrometer. The actual Re loadings of the catalysts were 1.53, 2.51, and 3.30 wt %, respectively. TPR was conducted on a Micrometrics AutoChem II chemisorption analyzer that used a moisture removal step. The moisture removal was conducted by ramping from room temperature to 120 °C in a He atmosphere at a rate of 10 °C/min and then holding at 120 °C for 1 h. After the hour hold, the sample was cooled to 40 °C at a rate of 10 °C/min. The gas environment was then switched to a 10% H_2 in Ar mixture and held for 30 min. After the 30 min the TPR experimentation was started by ramping from 40 to 800 °C at a rate of 5 °C/min with the detector recording a data point every second. After the program was completed, the gas flow was switched to He to purge the H_2 and cooled to 25 °C at a rate of 20 °C/min. The 2 and 3 wt % catalysts showed two distinct reduction peaks in the TPR spectra, with the 3 wt % catalyst used in the AHERY design having the lowest reduction temperatures as shown in Figure 1 Supplemental. The 4 wt % catalysts have broader reduction peaks in the TPR spectra which are at higher temperatures relative to the distinct reduction peaks seen in the 2 wt % catalysts.

DOI: 10.1021/acs.iecr.9b01463
Ind. Eng. Chem. Res. 2019, 58, 8681−8689

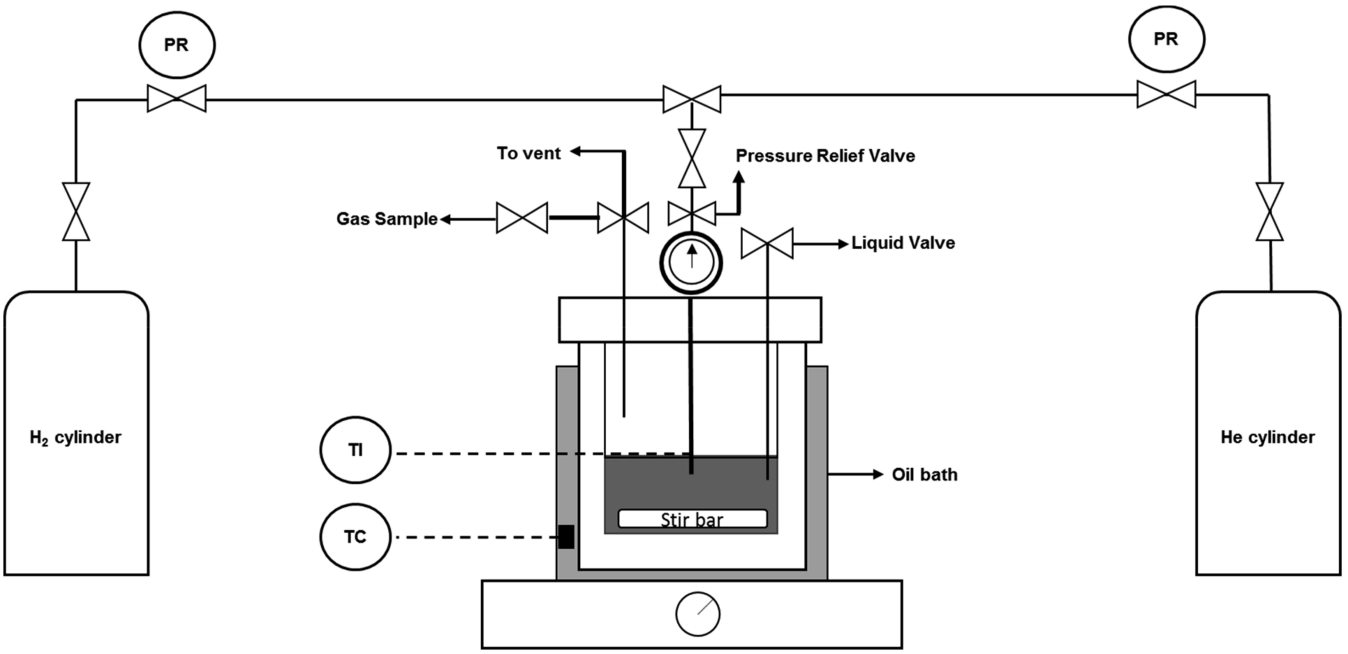

Figure 1. High pressure batch reactor system schematic.

Design of Experiments. An L9 Taguchi design was selected to investigate the effects of temperature, pressure, and catalyst loading on the yield of the AHERY S-HDO to help elucidate the optimum settings for the reaction and the effects of the various factors. A Taguchi design is a type of statistical design of experiment that aims to maximize a certain response based on the input variables it is given. For this work we used the input variables of temperature, pressure, and Re loading to try to maximize the yield of the S-HDO reactions. Each input variable utilized three evenly spaced levels to ensure the design was valid. Based on the number of input variables and the number of levels tested, the Taguchi design will elucidate how many experimental runs are necessary. A major benefit of a Taguchi design is that it drastically reduces the necessary experimental runs and associated costs.[29] The Taguchi design reduces the experimental runs due to the utilization of orthogonal arrays. Since the design utilizes orthogonal arrays, one of the potential drawbacks of a Taguchi design is that it gives only linear correlations for the various factors. However, the linear model equations fit our data quite well. The Taguchi design utilized temperatures of 100, 140, and 180 °C; pressures of 40, 60, and 80 bar H_2; and Re loadings of 2, 3, and 4 wt %. The full design layout can be seen in Table 2 Supplemental.

From the results of the AHERY S-HDO Taguchi design and various pressure sweeps, a similar 3 factor 3 level Taguchi design was constructed and tested for the xylitol reaction. The design tested temperatures of 140, 160, and 180 °C; pressures of 5, 7.5, and 10 bar H_2; and Re loadings of 2, 3, and 4 wt %. The full design layout can be seen in Table 3 Supplemental.

Reactor Setup and Mass Transfer Evaluation. A home-built 150 mL stainless steel high-pressure batch reactor was used for the AHERY S-HDO. The reactor schematic can be seen in Figure 1. The 150 mL reactor was machined from 316 SS. The base has a 2 in. diameter drilled out of a 3 in. diameter rod, leaving a 0.5 in. wall and bottom. Six holes were tapped in the top of the vessel for a bolted closure, and a groove was made for proper placement of an O-ring. The lid assembly was designed to permit both liquid and gas sampling through respective valves. The gas and liquid sampling valves allow for the various phases to be sampled during the reaction without the need to cool down or depressurize the reactor. The lid assembly was machined from a 0.5 in. thick 316 SS disk with 4 in. diameter, and the disk was tapped with 0.25 in. National Pipe Tapered (NPT) fittings. A pressure gauge was connected to one of the NPT taps. The other connections were made using bore through adapters with 0.25 in. male NPT and 0.125 in. male tube fittings. The various connections include a gas sampling/venting tube, liquid sampling tube, gas inlet valve, and thermocouple well. The reactor was placed in an oil bath for heating coupled with a PID controller to maintain temperature throughout the reaction. The internal reaction temperature is monitored with a K-type thermocouple that is inserted in the thermocouple well. A stir plate and 1.5 in. magnetic stir bar within the reactor were used for mixing. The reactor was pressure tested up to 100 bar and temperatures in excess of 150 °C. The gas sampling tube is equipped with a check valve to prevent air from entering the reactor after it has been purged. As a safety measure, a spring actuated pressure release valve was attached to the gas inlet.

To ensure that our reactor and stirring method was not mass transfer limited, a model reaction was chosen for validation. The hydrogenation of 2-methyl-3-butyn-2-ol (MBY) using a Lindlar catalyst is a well-studied and modeled reaction in the literature.[30−32] MBY is hydrogenated to 2-methyl-3-buten-2-ol (MBE), which is further hydrogenated to 2-methyl-2-butanol (MBA). Stirring rates ranging from 250 to 800 rpm were evaluated under 9 bar_g H_2 and 333 K for comparison to the rate constants, product profiles, and models proposed in the literature.[30] The study used for comparison utilized a gas entrainment impeller for mixing and gas introduction. Our reactor setup utilizes a simplistic magnetic stir bar for mixing and a gas inlet stream. In each reaction, the ratio of catalyst to liquid reactant was kept constant at 0.175 wt % as reported in the literature, where a rate of 5.8×10^{-2} mol/L/min was measured. For our reactor, following the procedure reported in the literature, the average reaction rate obtained was 5.8 ×

DOI: 10.1021/acs.iecr.9b01463
Ind. Eng. Chem. Res. 2019, 58, 8681−8689

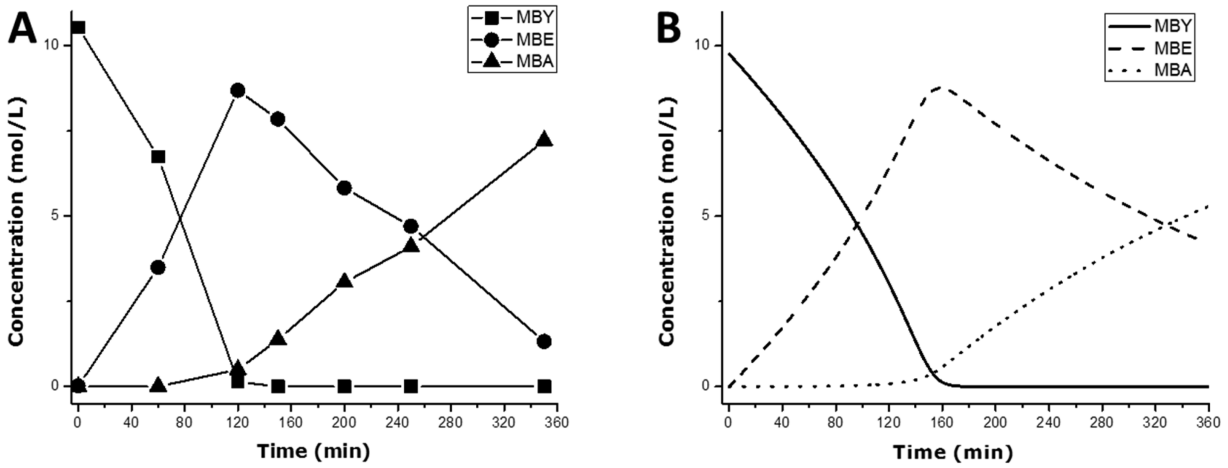

Figure 2. Mass transfer evaluation of the home-built reactor via the hydrogenation of MBY. (A) MBY hydrogenation reaction profile with stir rate of 550 rpm. (B) Model results from the literature[30] using P = 9 bar gauge, T = 333 K, and catalyst to reactant ratio = 0.175 wt %.

10^{-2} ± 0.002 mol/L/min, which is consistent with the previously reported values. For stir rates of 700 rpm and above, only 30% of the reactions were successful due to the stir bar losing the magnetic coupling. For stir rates of 250−450 rpm the reaction rate was lower than the previously reported reaction rate. Thus, the optimal range to conduct reactions in our reactor is between 550 and 650 rpm. The reaction profiles, as shown in Figure 2A, are also very consistent with the model results from the literature, shown in Figure 2B. In conclusion, the reproducibility of the reaction rates and the concentration profiles and their similarity with previously reported literature show that our reactor is not controlled by external mass transfer limitations for stir rates of 550 rpm and above. Therefore, all reactions were performed at 550 rpm.

Activity Measurements. *AHERY Reactions.* The AHERY S-HDO was used as a model reaction for sugar alcohol S-HDO. The hydrogen was added initially at room temperature to the reactant, solvent, and catalyst mixture, which was then heated to the desired temperature. The reaction time was started once the reactor reached the desired temperature. Each reaction contained 50 mL of 1,4-dioxane (solvent), 3.15 mL (4 g) of AHERY, and 0.60 g of ReO_x−Pd/CeO_2 catalyst. The ratio of catalyst to reactant previously suggested in the literature of 1 g of AHERY:0.15 g of ReO_x−Pd/CeO_2 catalyst was followed.[5] Liquid samples were taken at the initial and final points of the reaction. The samples were diluted in methanol to $\frac{125}{3}$ of their original volume and analyzed in a Shimadzu GC-2010 Plus. The gas chromatograph (GC) utilized a flame ionization detector, an RTX-1701 column, and an AOC-5000 autoinjector. The GC was calibrated for AHERY and THF. For the AHERY S-HDO, conversion is based on the final and initial concentrations of AHERY. The selectivity to THF was calculated based on moles of THF produced with respect to the total moles of products produced. The only other product that was observed in the GC analysis was *trans*-AHERY. The yield of the AHERY S-HDO was calculated by taking the product of the AHERY conversion and the THF selectivity.

Xylitol Reactions. For the xylitol reactions, the reactor was filled with the reaction mixture and heated to the desired temperature. After the desired temperature was reached, constant hydrogen pressure was introduced and maintained. Each reaction contained 50 mL of 1,4-dioxane (solvent), 2 g of xylitol, and 0.60 g of ReO_x−Pd/CeO_2 catalyst, again following the literature.[12] Liquid samples were taken at the initial point, midpoint, and final point of the reaction. The samples were again diluted to $\frac{125}{3}$ of their original volume and analyzed by GC. The GC was calibrated for xylitol, 1,2-dideoxypentitol, 1,2,5-pentanetriol, 3-pentanol, 1-pentanol, and 1,2-pentanediol. For the xylitol S-HDO, conversion was calculated based on the concentration of the products formed and their theoretical maximums. The selectivity of 1,2-dideoxypentitol and 1,2,5-pentanetriol (1 S-HDO products) was calculated based on the moles of the 1 S-HDO products produced with respect to the total moles of all products formed. The yield of the 1 S-HDO products was calculated by taking the product of the xylitol conversion and the 1 S-HDO selectivity.

RESULTS AND DISCUSSION

AHERY S-HDO L9 Taguchi Design. The results from each experimental run of the Taguchi design are shown in Table 1. To ensure the results were reproducible, a center point of the design with the conditions of 60 bar H_2, 140 °C, and a 4 wt % Re catalyst was repeated three times. As shown in Table 4 Supplemental, the standard errors between runs were 0.97 and 0.20% for conversion and selectivity, respectively. The yield of the reactions had a standard error of 0.92%, which is shown in Table 4 Supplemental. The standard errors for conversion, selectivity, and yield were calculated using the formula SE=$\frac{\sigma}{\sqrt{n}}$, where SE is standard error, σ is the standard

Table 1. AHERY Model Reaction DOE Results

press. (bar)	temp (°C)	Re loading (wt %)	conv (%)	THF selectivity (%)
40	100	2	14.5	75.0
40	140	3	30.7	95.5
40	180	4	99.9	99.7
60	100	3	3.93	99.9
60	140	4	21.3	99.9
60	180	2	99.9	98.0
80	100	4	3.63	99.9
80	140	2	21.7	99.9
80	180	3	75.0	99.9

DOI: 10.1021/acs.iecr.9b01463
Ind. Eng. Chem. Res. 2019, 58, 8681−8689

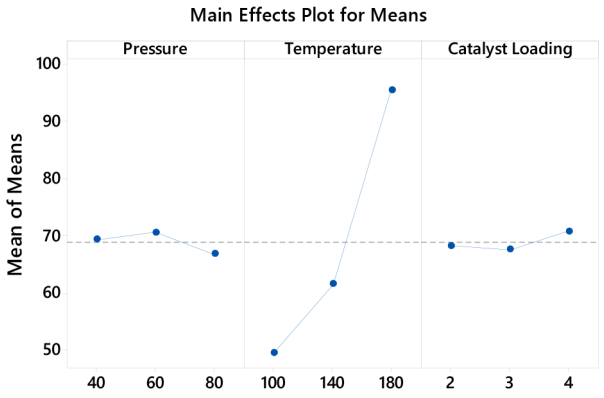

Figure 3. Correlation between design factors and responses resulting from L9 Taguchi design of experiments.

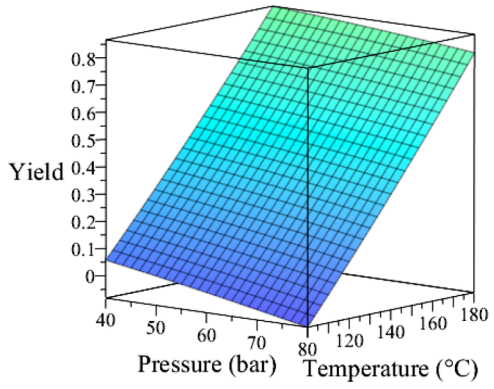

Figure 5. Three-dimensional yield contour for the S-HDO of AHERY using a 3 wt % ReO_x−Pd/CeO_2 catalyst and Taguchi model equations.

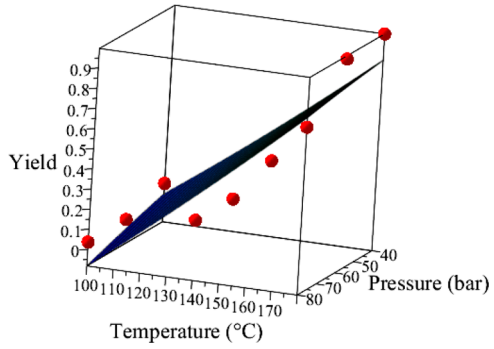

Figure 6. Yield contour overlaying experimental data points from the AHERY Taguchi design.

deviation of the three experimental data points, and n is the population size, which was 3 in these cases.

The main effects plot shows how the factors in the design affect the desired responses and thus how significant they are. The larger the slope of the line, the more statistically significant the factor. Temperature is the most significant factor in this process and has the strongest effect on the yield of the reaction, according to its slope shown in Figure 3. Catalyst loading was found to be mildly significant, but compared to the temperature it had a small effect on the reaction. However, the pressure of the reaction was statistically insignificant, since there was no obvious correlation between the data points and the slope of the line was very small. The lack of dependence on pressure suggests that we have a zero-order relation on hydrogen pressure for this reaction. Thus, the deoxydehydration step of this reaction is likely the rate-limiting step. The

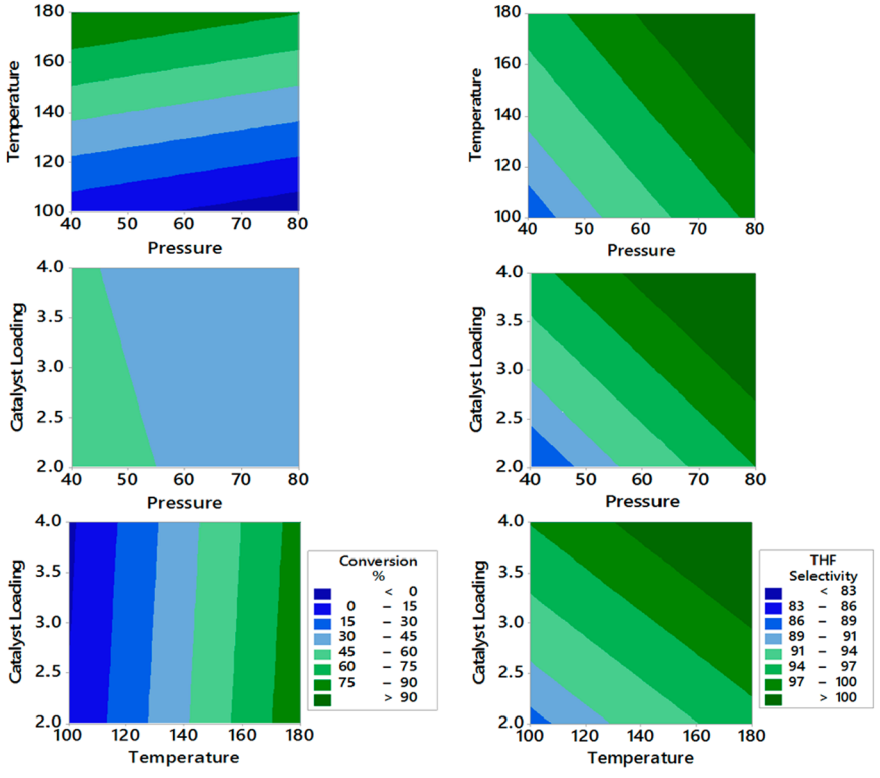

Figure 4. Taguchi model regression contours for conversion and selectivity for AHERY S-HDO.

DOI: 10.1021/acs.iecr.9b01463
Ind. Eng. Chem. Res. 2019, 58, 8681−8689

Table 2. Xylitol Reaction DOE Results

press. (bar)	temp (°C)	Re loading (wt %)	conv (%)	1 S-HDO selectivity (%)
5	140	2	26.5	99.9
5	160	3	25.8	99.9
5	180	4	0	0
7.5	140	3	33.9	99.9
7.5	160	4	39.7	68.2
7.5	180	2	33.0	99.9
10	140	4	56.6	88.3
10	160	2	56.3	93.7
10	180	3	32.1	99.9

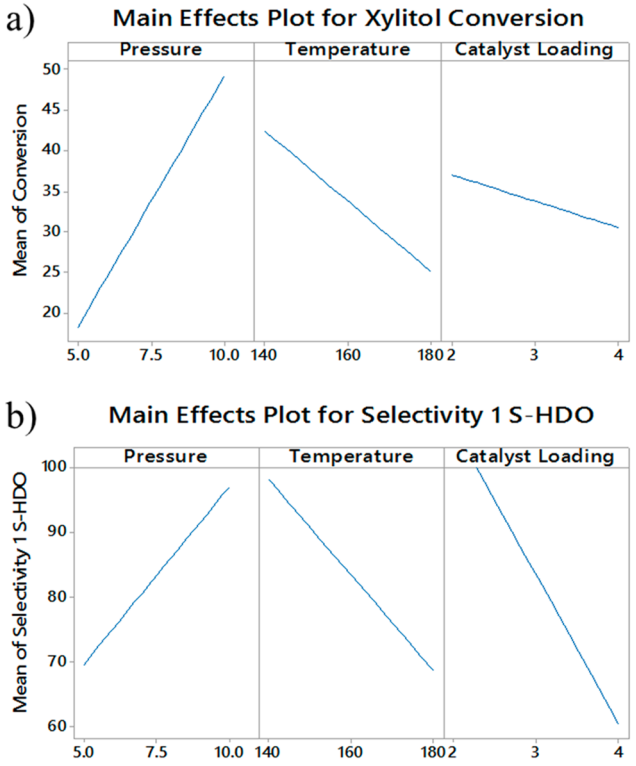

Figure 7. Correlation between design factors and responses resulting from the xylitol L9 Taguchi design of experiments. (a) Conversion correlations. (b) Selectivity to 1,2-dideoxypentitol and 1,2,5-pentanetriol correlations.

deoxydehydration of AHERY produces 2,5-dihydrofuran,[33] which is not observed during our analysis. The Pd on the surface of the CeO_2 catalyzes hydrogen dissociation and spillover on the CeO_2 which allows for the regeneration of the catalyst.[34] Thus, the surface of the catalyst may be saturated with hydrogen and the hydrogenation step proceeds as soon as the deoxydehydration step is completed.

Since the Taguchi design creates linear models, it is important to look at the proportionality of the factors and investigate if there are regions where certain conditions are more favorable. When looking at the yield of this reaction, the individual factors can affect conversion and selectivity differently. The varying proportionality can result in regions that are more favorable for higher yield. The proportionality of the various factors is shown in the various contours created by the regression of the Taguchi model shown in Figure 4. The temperature of the reaction is directly related to both conversion and selectivity. The temperature is thus directly related to the yield of the AHERY S-HDO and thus should be high to increase the yield of the reaction. The pressure was found to be inversely related to conversion, but directly related to selectivity.

In order to see where the varying proportionality of pressure is most favorable, a yield contour over varying pressures was investigated using the Taguchi model equations to form a three-dimensional (3D) yield contour, as shown in Figure 5. The Taguchi model equations for conversion and selectivity are shown in Table 5 Supplemental. In order to construct the 3D yield contour, one dimension must be reduced in order to plot the figure. Catalyst loading was chosen as the dimension to reduce since it was found to have a small impact on the yield, and the goal of the design was to find milder reaction conditions. The center point of catalyst loading, 3 wt %, was chosen to ensure the model equations would not be skewed. Reducing the pressure to 40 bar slightly improves the yield of the reaction. The pressure effects on conversion and selectivity seem to be negligible in the higher temperature region of our design but can become somewhat significant at lower temperatures. This adds further support to the reduction of pressure having negligible effects on the yield of AHERY S-HDO. Based on the model equations and the yield contour resulting from them, the optimal reaction conditions within the design space are 40 bar and 180 °C.

Even though the yield contour results from linear model equations, it captures the general trends of the design space, as shown in Figure 6. The relatively close fitting of the data points further confirms the validity of the Taguchi model equations resulting from the AHERY S-HDO.

In summary, we have shown that milder reaction conditions for the S-HDO of AHERY are feasible with respect to pressure, and the ability to reduce the pressure without causing a decline in yield has been demonstrated. This reaction can serve as a model for other lignocellulosic biomass S-HDO reactions and suggests that reducing the pressure might not have a significant effect on yield. Since the temperature has a significant effect on yield, it would be optimal to run S-HDO reactions at higher temperatures. To see if these statements hold for another sugar alcohol, we performed a similar design for xylitol.

Pressure Effects on the Xylitol Reaction. For the AHERY S-HDO, the pressure region above 40 bar was shown to have a zero-order dependence on yield. Pressures of 40 bar and below were investigated for the xylitol S-HDO to discover the threshold below which pressure starts to affect this reaction. Pressures of 40, 10, 7.5, and 5 bar were evaluated using a 4 wt % ReO_x−Pd/CeO_2 catalyst at 160 °C. The results from these reactions are shown in Table 6 Supplemental. For pressures of 10 bar and below, the reactor was loaded with catalyst, solvent, and reactant and then brought to the desired reaction temperature before H_2 was introduced. The most significant change occurred within the 5−10 bar region. The calculated yield refers to the most valuable products 1,2-dideoxypentitol and 1,2,5-pentanetriol, which are formed through 1 S-HDO. The selectivity to 1,2-dideoxypentitol and 1,2,5-pentanetriol for the 40 and 10 bar reactions were the same within experimental error. However, the conversion for the 10 bar reactions were significantly higher, thus resulting in a higher yield. Below 10 bar, there is a significant drop in activity for the xylitol S-HDO. The reactions at 7.5 and 5 bar only obtained 42.6 and 33.3% of the yield that the reaction produced at 10 bar. To further investigate this change in yield

DOI: 10.1021/acs.iecr.9b01463
Ind. Eng. Chem. Res. 2019, 58, 8681−8689

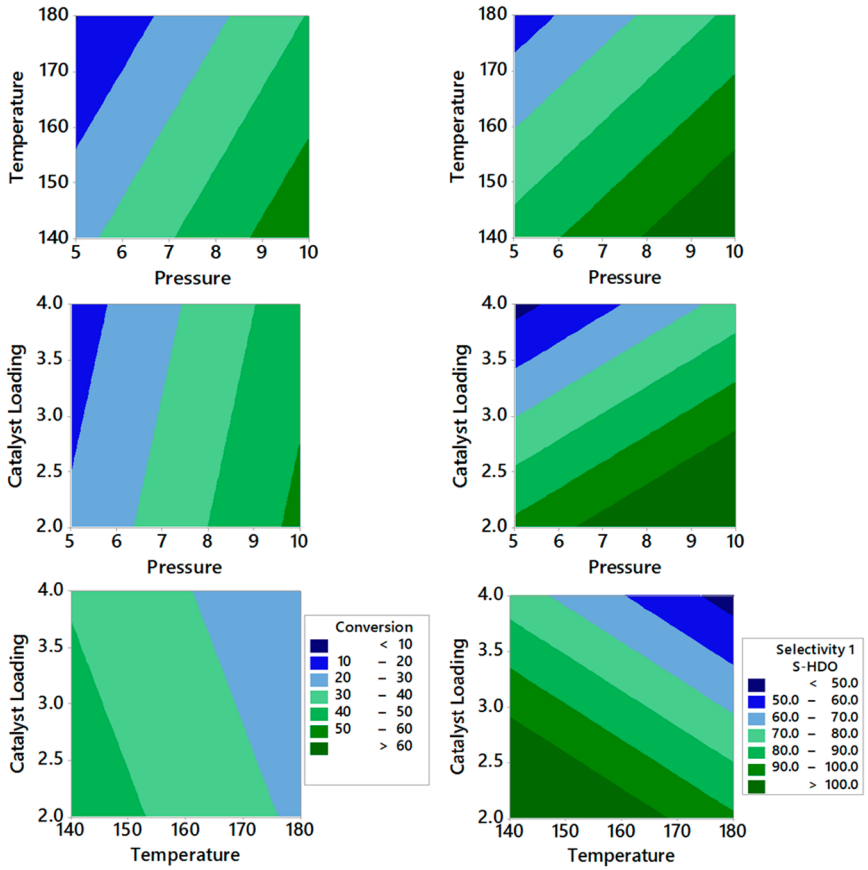

Figure 8. Taguchi model regression contours for the conversion and selectivity for xylitol S-HDO.

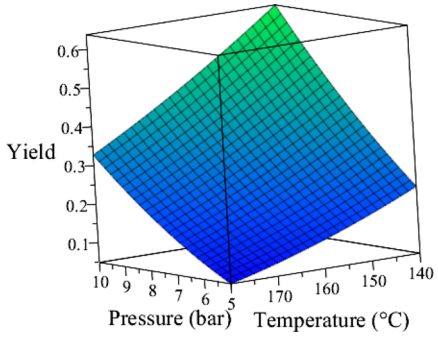

Figure 9. Three-dimensional yield contour for the S-HDO of xylitol via a 3 wt % ReO_x−Pd/CeO_2 catalyst using Taguchi model equations.

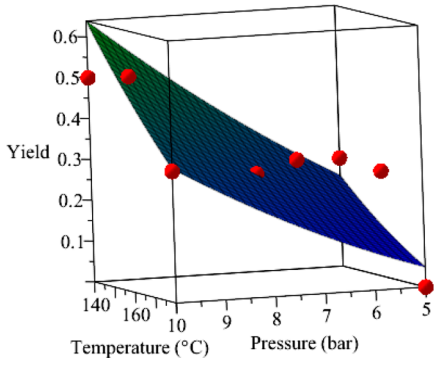

Figure 10. Yield contour overlaying experimental data points from the xylitol Taguchi design.

with respect to pressure, the L9 Taguchi design for the xylitol S-HDO included the factor of pressure with levels between 5 and 10 bar H_2.

Xylitol S-HDO L9 Taguchi Design. The results from each experimental run of the Taguchi design are shown in Table 2. To ensure the results were reproducible, a center point of the design with conditions of 7.5 bar H_2, 140 °C, and a 3 wt % Re catalyst was repeated three times. As shown in Table 7 Supplemental, the standard errors between the runs were 4.71 and 1.77% for xylitol conversion and selectivity to the 1 S-HDO products, respectively. The yield of 1 S-HDO products for the reactions had a standard error of 3.86% which is shown in Table 7 Supplemental. The standard errors were calculated as previously described in the AHERY design.

The main effect plots for the conversion of xylitol and the selectivity to the products which have undergone 1 S-HDO are shown in Figure 7. For both conversion and selectivity, pressure exhibits a direct relation and temperature and catalyst loading have inverse relations within the design space. Although the relations agree, the scale of the relations is different. The factors affect selectivity significantly more than they affect conversion. The relations of the factors for the xylitol design vary from the model AHERY design. The most significant difference is in the relation of temperature. A stronger effect of catalyst loading on conversion and selectivity has also been noted. The 2 wt % ReO_x−Pd/CeO_2 catalyst was superior to the 3 and 4 wt % catalysts in terms of both conversion and selectivity in the xylitol S-HDO.

DOI: 10.1021/acs.iecr.9b01463
Ind. Eng. Chem. Res. 2019, 58, 8681−8689

In the conversion and selectivity contour plots for the xylitol S-HDO, shown in Figure 8, it is further displayed that the relations of the various factors follow the same proportionality.

In order to see how the factors affect the yield of the xylitol S-HDO, a 3D yield contour plot was constructed, as shown in Figure 9. The Taguchi model equations used to construct the 3D contour are shown in Table 8 Supplemental. The 3D yield contour was constructed by reducing a dimension, as previously mentioned for the AHERY S-HDO contour. Catalyst loading was the dimension reduced, and the center point of 3 wt % was chosen so that reaction conditions could be evaluated. The yield contour suggests that the optimal reaction conditions for the xylitol S-HDO are 140 °C and 10 bar within the design space tested. These optimal conditions are significantly milder if compared to the previously reported 160 °C and 80 bar.[12]

The yield contour was overlaid with the experimental data points, as shown in Figure 10 to illustrate how the model equations fit the data. The Taguchi model equations fit the experimental points well for a linear model but do not completely capture the trends in the studied parameter space. One of the drawbacks of a Taguchi design is that it will not capture higher order interactions between factors, which might lead to the observed difference between the model and the experimental data points.[35,36]

CONCLUSIONS

This work elucidated that the reduction of pressure for the AHERY S-HDO process from 80 to 40 bar H_2 while using a ReO_x–Pd/CeO_2 catalyst maintained a similar yield of THF. For the xylitol S-HDO, the optimal conditions were found to be 140 °C and 10 bar H_2 within the design space, conditions that are substantially lower than those previously reported in the literature.[12] Yield was found to have a zero-order relation for pressures as low as 10 bar for the xylitol S-HDO. These optimal and milder reaction conditions allow for 1,2-dideoxypentitol and 1,2,5-pentanetriol to be produced in a more economically feasible approach, allowing for the production of platform and value-added chemicals from a renewable feedstock.

ASSOCIATED CONTENT

Supporting Information

The Supporting Information is available free of charge on the ACS Publications website at DOI: 10.1021/acs.iecr.9b01463.

Chemical list, catalyst characterization, AHERY Taguchi design, xylitol Taguchi design, AHERY design reproducibility, AHERY Taguchi model equations, pressure effects on xylitol S-HDO, xylitol design reproducibility, xylitol Taguchi model equations (PDF)

AUTHOR INFORMATION

Corresponding Author

*E-mail: lauteraj@cec.sc.edu.

ORCID

Andreas Heyden: 0000-0002-4939-7489

Jochen Lauterbach: 0000-0001-8303-7703

Notes

The authors declare no competing financial interest.

ACKNOWLEDGMENTS

We gratefully acknowledge financial support from the National Science Foundation (OIA-1632824 and DGE-1250052). This work was also supported by the South Carolina Smart State Center for Strategic Approaches to the Generation of Electricity (SAGE).

REFERENCES

(1) Alonso, D. M.; Wettstein, S. G.; Dumesic, J. A. Bimetallic Catalysts for Upgrading of Biomass to Fuels and Chemicals. *Chem. Soc. Rev.* **2012**, *41* (24), 8075–8098.

(2) Melin, K.; Hurme, M. Evaluation of Lignocellulosic Biomass Upgrading Routes To Fuels and Chemicals. *Cellul. Chem. Technol.* **2010**, *44* (4–6), 117–137.

(3) Luterbacher, J. S.; Martin Alonso, D.; Dumesic, J. A. Targeted Chemical Upgrading of Lignocellulosic Biomass to Platform Molecules. *Green Chem.* **2014**, *16* (12), 4816–4838.

(4) Amada, Y.; Ota, N.; Tamura, M.; Nakagawa, Y.; Tomishige, K. Selective Hydrodeoxygenation of Cyclic Vicinal Diols to Cyclic Alcohols over Tungsten Oxide-Palladium Catalysts. *ChemSusChem* **2014**, *7* (8), 2185–2192.

(5) Ota, N.; Tamura, M.; Nakagawa, Y.; Okumura, K.; Tomishige, K. Performance, Structure, and Mechanism of ReO_x – Pd/CeO_2 Catalyst for Simultaneous Removal of Vicinal OH Groups with H_2. *ACS Catal.* **2016**, *6* (5), 3213–3226.

(6) Stalpaert, M.; De Vos, D. Stabilizing Effect of Bulky *β*-Diketones on Homogeneous Mo Catalysts for Deoxydehydration. *ACS Sustainable Chem. Eng.* **2018**, *6*, 12197–12204.

(7) Tazawa, S.; Ota, N.; Tamura, M.; Nakagawa, Y.; Okumura, K.; Tomishige, K. Deoxydehydration with Molecular Hydrogen over Ceria-Supported Rhenium Catalyst with Gold Promoter. *ACS Catal.* **2016**, *6* (10), 6393–6397.

(8) Wang, T.; Liu, S.; Tamura, M.; Hiyoshi, N.; Tomishige, K.; Nakagawa, Y. One-Pot Catalytic Selective Synthesis of 1,4-butanediol from 1,4–anhydroerythritol and hydrogen. *Green Chem.* **2018**, *20*, 2547–2557.

(9) Tamura, M.; Yuasa, N.; Cao, J.; Nakagawa, Y.; Tomishige, K. Heterogeneous Catalysis Transformation of Sugars into Chiral Polyols over a Heterogeneous Catalyst. *Angew. Chem., Int. Ed.* **2018**, *57*, 8058–8062.

(10) Cao, J.; Tamura, M.; Nakagawa, Y.; Tomishige, K. Direct Synthesis of Unsaturated Sugars from Methyl Glycosides. *ACS Catal.* **2019**, *9*, 3725–3729.

(11) Shakeri, J.; Hadadzadeh, H.; Farrokhpour, H.; Weil, M. A Comparative Study of the Counterion Effect on the Perrhenate-Catalyzed Deoxydehydration Reaction. *Mol. Catal.* **2019**, *471*, 27–37.

(12) Ota, N.; Tamura, M.; Nakagawa, Y.; Okumura, K.; Tomishige, K. Hydrodeoxygenation of Vicinal OH Groups over Heterogeneous Rhenium Catalyst Promoted by Palladium and Ceria Support. *Angew. Chem., Int. Ed.* **2015**, *54* (6), 1897–1900.

(13) Zhao, C.; He, J.; Lemonidou, A. A.; Li, X.; Lercher, J. A. Aqueous-Phase Hydrodeoxygenation of Bio-Derived Phenols to Cycloalkanes. *J. Catal.* **2011**, *280* (1), 8–16.

(14) Şenol, O. İ.; Viljava, T.-R.; Krause, A. O. I. Hydrodeoxygenation of Methyl Esters on Sulphided NiMo/*γ*-Al2O3 and CoMo/*γ*-Al2O3 Catalysts. *Catal. Today* **2005**, *100* (3–4), 331–335.

(15) Gutierrez, A.; Kaila, R. K.; Honkela, M. L.; Slioor, R.; Krause, A. O. I. Hydrodeoxygenation of Guaiacol on Noble Metal Catalysts. *Catal. Today* **2009**, *147* (3–4), 239–246.

(16) Zhao, C.; Kou, Y.; Lemonidou, A. A.; Li, X.; Lercher, J. A. Hydrodeoxygenation of Bio-Derived Phenols to Hydrocarbons Using RANEY® Ni and Nafion/SiO2 Catalysts. *Chem. Commun.* **2010**, *46* (3), 412–414.

(17) Centeno, A.; Laurent, E.; Delmon, B. Influence of the Support of CoMo Sulfide Catalysts and of the Addition of Potassium and Platinum on the Catalytic Performances for the Hydrodeoxygenation of Carbonyl, Carboxyl, and Guaiacol-Type Molecules. *J. Catal.* **1995**, *154*, 288–298.

DOI: 10.1021/acs.iecr.9b01463
Ind. Eng. Chem. Res. 2019, 58, 8681–8689

(18) Lee, C. R.; Yoon, J. S.; Suh, Y. W.; Choi, J. W.; Ha, J. M.; Suh, D. J.; Park, Y. K. Catalytic Roles of Metals and Supports on Hydrodeoxygenation of Lignin Monomer Guaiacol. *Catal. Commun.* **2012**, *17*, 54−58.
(19) Prasomsri, T.; Nimmanwudipong, T.; Román-Leshkov, Y. Effective Hydrodeoxygenation of Biomass-Derived Oxygenates into Unsaturated Hydrocarbons by MoO3 Using Low H2 Pressures. *Energy Environ. Sci.* **2013**, *6* (6), 1732−1738.
(20) Saha, B.; Bohn, C. M.; Abu-Omar, M. M. Zinc-Assisted Hydrodeoxygenation of Biomass-Derived 5-Hydroxymethylfurfural to 2,5-Dimethylfuran. *ChemSusChem* **2014**, *7* (11), 3095−3101.
(21) Laskar, D. D.; Tucker, M. P.; Chen, X.; Helms, G. L.; Yang, B. Noble-Metal Catalyzed Hydrodeoxygenation of Biomass-Derived Lignin to Aromatic Hydrocarbons. *Green Chem.* **2014**, *16* (2), 897−910.
(22) Grilc, M.; Veryasov, G.; Likozar, B.; Jesih, A.; Levec, J. Hydrodeoxygenation of Solvolysed Lignocellulosic Biomass by Unsupported MoS2, MoO2, Mo2C and WS2catalysts. *Appl. Catal., B* **2015**, *163*, 467−477.
(23) Bu, Q.; Lei, H.; Zacher, A. H.; Wang, L.; Ren, S.; Liang, J.; Wei, Y.; Liu, Y.; Tang, J.; Zhang, Q.; et al. A Review of Catalytic Hydrodeoxygenation of Lignin-Derived Phenols from Biomass Pyrolysis. *Bioresour. Technol.* **2012**, *124*, 470−477.
(24) Ren, H.; Yu, W.; Salciccioli, M.; Chen, Y.; Huang, Y.; Xiong, K.; Vlachos, D. G.; Chen, J. G. Selective Hydrodeoxygenation of Biomass-Derived Oxygenates to Unsaturated Hydrocarbons Using Molybdenum Carbide Catalysts. *ChemSusChem* **2013**, *6* (5), 798−801.
(25) Nakagawa, Y.; Liu, S.; Tamura, M.; Tomishige, K. Catalytic Total Hydrodeoxygenation of Biomass-Derived Polyfunctionalized Substrates to Alkanes. *ChemSusChem* **2015**, *8* (7), 1114−1132.
(26) Wang, L.; Weng, Y.; Duan, P.; Liu, X.; Wang, X.; Zhang, Y.; Wang, C.; Liu, Q.; Ma, L. Influence of Acid Pretreatment on the Hydrodeoxygenation Performance of Carbon Supported RuMo Bimetallic Catalysts on Sorbitol Conversion. *SN Appl. Sci.* **2019**, *1*, 404.
(27) Jin, X.; Yin, B.; Xia, Q.; Fang, T.; Shen, J.; Kuang, L.; Yang, C. Catalytic Transfer Hydrogenation of Biomass-Derived Substrates to Value-Added Chemicals on Dual-Function Catalysts: Opportunities and Challenges. *ChemSusChem* **2019**, *12*, 71−92.
(28) Venkateswar Rao, L.; Goli, J. K.; Gentela, J.; Koti, S. Bioconversion of Lignocellulosic Biomass to Xylitol: An Overview. *Bioresour. Technol.* **2016**, *213*, 299−310.
(29) Ballantyne, K. N.; van Oorschot, R. A.; Mitchell, R. J. Reduce Optimisation Time and Effort: Taguchi Experimental Design Methods. *Forensic Sci. Int. Genet. Suppl. Ser.* **2008**, *1* (1), 7−8.
(30) Vernuccio, S.; Von Rohr, P. R.; Medlock, J. General Kinetic Modeling of the Selective Hydrogenation of 2-Methyl-3-Butyn-2-Ol over a Commercial Palladium-Based Catalyst. *Ind. Eng. Chem. Res.* **2015**, *54* (46), 11543−11551.
(31) Bruehwiler, A.; Semagina, N.; Grasemann, M.; Renken, A.; Kiwi-Minsker, L.; Saaler, A.; Lehmann, H.; Bonrath, W.; Roessler, F. Three-Phase Catalytic Hydrogenation of a Functionalized Alkyne: Mass Transfer and Kinetic Studies with in Situ Hydrogen Monitoring. *Ind. Eng. Chem. Res.* **2008**, *47* (18), 6862−6869.
(32) Crespo-Quesada, M.; Grasemann, M.; Semagina, N.; Renken, A.; Kiwi-Minsker, L. Kinetics of the Solvent-Free Hydrogenation of 2-Methyl-3-Butyn-2-Ol over a Structured Pd-Based Catalyst. *Catal. Today* **2009**, *147* (3−4), 247−254.
(33) Sandbrink, L.; Beckerle, K.; Meiners, I.; Liffmann, R.; Rahimi, K.; Okuda, J.; Palkovits, R. Supported Molybdenum Catalysts for the Deoxydehydration of 1,4-Anhydroerythritol into 2,5-Dihydrofuran. *ChemSusChem* **2017**, *10* (7), 1375−1379.
(34) Xi, Y.; Yang, W.; Ammal, S. C.; Lauterbach, J.; Pagan-Torres, Y.; Heyden, A. Mechanistic Study of the Ceria Supported, Re-Catalyzed Deoxydehydration of Vicinal OH Groups. *Catal. Sci. Technol.* **2018**, *8* (22), 5750−5762.
(35) Engel, J.; Huele, A. F. Taguchi Parameter Design by Second-Order Response Surfaces. *Qual. Reliab. Eng. Int.* **1996**, *12*, 95−100.
(36) Parks, J. M. On Stochastic Optimization: Taguchi Methods Demystified ; Its Limitations and Fallacy Clarified. *Probabilistic Eng. Mech.* **2001**, *16*, 87−101.

DOI: 10.1021/acs.iecr.9b01463
Ind. Eng. Chem. Res. 2019, 58, 8681−8689